Title

Free-water and free-water corrected fractional anisotropy in primary and premotor corticospinal tracts in chronic stroke

Journal

Human Brain Mapping, 38(9)

ISSN

1065-9471

Authors

Archer, Derek B
Patten, Carolynn
Coombes, Stephen A

Publication Date

2017-09-01

DOI

10.1002/hbm.23681

Peer reviewed

◆ Human Brain Mapping 38:4546–4562 (2017) ◆

Free-Water and Free-Water Corrected Fractional Anisotropy in Primary and Premotor Corticospinal Tracts in Chronic Stroke

Derek B. Archer,[1] **Carolynn Patten**,[2,3,4] **and Stephen A. Coombes**[1]*

[1]*Laboratory for Rehabilitation Neuroscience, Department of Applied Physiology and Kinesiology, University of Florida, Gainesville, Florida*
[2]*Rehabilitation Sciences Ph.D. Program, Department of Physical Therapy, University of Florida, Gainesville, Florida*
[3]*Neural Control of Movement Lab, Malcolm Randall VA Medical Center, Gainesville, Florida*
[4]*Department of Neurology, University of Florida, Gainesville, Florida*

Abstract: Measures from diffusion MRI have been used to characterize the corticospinal tract in chronic stroke. However, diffusivity can be influenced by partial volume effects from free-water, region of interest placement, and lesion masking. We collected diffusion MRI from a cohort of chronic stroke patients and controls and used a bitensor model to calculate free-water corrected fractional anisotropy (FA_T) and free water (FW) in the primary motor corticospinal tract (M1-CST) and the dorsal premotor corticospinal tract (PMd-CST). Region of interest analyses and whole-tract slice-by-slice analyses were used to assess between-group differences in FA_T and FW in each tract. Correlations between FA_T and FW and grip strength were also examined. Following lesion masking and correction for multiple comparisons, relative increases in FW were found for the stroke group in large portions of the M1-CST and PMd-CST in the lesioned hemisphere. FW in cortical regions was the strongest predictor of grip strength in the stroke group. Our findings also demonstrated that FA_T is sensitive to the direct effects of the lesion itself, thus after controlling for the lesion, differences in FA_T in nonlesioned tissue were small and generally similar between hemispheres and groups. Our observations suggest that FW may be a robust biological measurement that can be used to assess microstructure in residual white matter after stroke. *Hum Brain Mapp 38:4546–4562, 2017.* **© 2017 Wiley Periodicals, Inc.**

Key words: chronic stroke; white matter tractography; rehabilitation; fractional anisotropy; corticospinal tract

INTRODUCTION

Brain lesions resulting from stroke lead to profound changes in behavior. For example, approximately 70% of stroke survivors live with deficits in upper extremity function [Nakayama, 1994; Tennant, 1997; Meyer, 2014]. Biomarkers for stroke recovery are needed to serve as surrogate indicators of disease state, predict recovery or treatment response, and move stroke rehabilitation research forward [Kim and Winstein, 2016]. In this study, we examine a novel dMRI measurement, termed free-water [Metzler-Baddeley et al., 2012; Reetz and Binkofski, 2013; Reetz et al., 2013],

*Correspondence to: Stephen A. Coombes, PhD; University of Florida, Laboratory for Rehabilitation Neuroscience, Department of Applied Physiology and Kinesiology, PO Box 118206, Florida, USA. E-mail: scoombes@ufl.edu

Received for publication 28 November 2016; Revised 8 May 2017; Accepted 26 May 2017.

DOI: 10.1002/hbm.23681

Published online 7 June 2017 in Wiley Online Library (wileyonlinelibrary.com).

which has not previously been studied in the context of chronic stroke.

The corticospinal motor tract (CST) is essential for voluntary motor function because it allows for the transfer of signals from the motor cortex to the distal upper-extremity musculature [Heffner and Masterton, 1983; Jang, 2009; Lemon and Griffiths, 2005; Nudo and Masterton, 1990a, 1990b]. Seminal studies conducted in nonhuman primates show that lesions to the CST produce deficits in motor function. Diffusion magnetic resonance imaging (dMRI) lesion studies in humans support this position [Archer et al., 2016; Dum and Strick, 1991; Groisser et al., 2014; He et al., 1993, 1995; Schaechter et al., 2008, 2009; Schulz et al., 2012; Thomalla et al., 2004].

Diffusion MRI is a useful tool to evaluate the CST in humans because it allows for the *in vivo* quantification of white matter microstructure [Jones et al., 2013]. Measures of microstructure such as fractional anisotropy (FA) can be derived from dMRI, and several groups have now shown that FA is reduced in specific regions of the CST in the chronic phase after stroke [Archer et al., 2016; Lindenberg et al., 2010, 2012; Stinear et al., 2007, 2012]. However, atrophy-based partial volume free-water (FW) contamination can bias the diffusion index which limits the utility of FA as a measure of tissue microstructure [Metzler-Baddeley et al., 2012; Reetz and Binkofski, 2013; Reetz et al., 2013]. FW dMRI analysis using a bi-tensor model has been developed to overcome this limitation [Metzler-Baddeley et al., 2012; Pasternak et al., 2009]. FW measurements provide an index of extracellular fluid within a voxel. When the FW component is eliminated, the remaining dMRI signal provides a corrected FA value (FA_T), which is generally higher compared to the original FA value [Pasternak et al., 2009]. FW is expected to increase with atrophy-based neurodegeneration [Pasternak et al., 2012a; Wang et al., 2011], and recent evidence shows that FW is sensitive to disease states such as schizophrenia and Parkinson's disease [Ofori et al., 2015; Pasternak et al., 2012b]. FW and FA_T measurements have not been examined in the CST in the chronic phase after stroke.

Changes in CST microstructure after stroke have been interpreted as reflecting Wallerian degeneration [DeVetten et al., 2010; Mazumdar et al., 2003], which follows a stereotypical course [Iizuka et al., 1989; Johnson et al., 1950; Lampert and Cressman, 1966]. Evidence from animal studies demonstrates that the disintegration of axonal structures and fragmentation of the myelin sheaths occurs within days after the infarct. Myelin degradation, which leads to fibrosis and atrophy of the affected tract due to the infiltration of astrocytes, emerges at approximately 14 days [Iizuka et al., 1989; Johnson et al., 1950; Lampert and Cressman, 1966]. In humans, the first studies to show deficits in microstructural properties of the CST drew regions of interest (ROIs) in the posterior limb of the internal capsule (PLIC) and cerebral peduncle (CP) using anatomical landmarks and FA maps to guide ROI placement [Lindenberg et al., 2010, 2012; Schaechter et al., 2008, 2009; Stinear et al., 2007; Thomalla et al., 2004]. Other studies have reported stroke related deficits in microstructure by averaging measures across the entire CST [Lindenberg et al., 2012]. What is not clear from these studies is whether chronic stroke is associated with both decreases in FA_T and increases in FW across all segments of the CST or whether differences are limited to the PLIC and CP. In contrast to dMRI studies that focus on PLIC and CP, functional MRI studies have characterized changes in the blood oxygenation level response (BOLD) in cortical motor regions in the chronic phase after stroke. Increased BOLD signal in contralesional M1 and bilateral PMd has been demonstrated during motor tasks performed by the impaired hand, and these data have been interpreted as reflecting cortical reorganization in primary and premotor areas [Buetefisch et al., 2014; Burke Quinlan et al., 2015; Loubinoux et al., 2007; Plow et al., 2015; Rehme et al., 2012; Tombari et al., 2004; Ward et al., 2003]. Here, we extend dMRI analyses to include cortical regions using both ROI- and slice-level approaches.

We calculated measures of FA_T and FW in the primary motor corticospinal tract (M1-CST) and the dorsal premotor corticospinal tract (PMd-CST). ROI analyses (CP, PLIC, and cortex) and slice-by-slice analyses were used to assess between group differences in FA_T and FW in the M1-CST and PMd-CST. Correlations between grip strength and FA_T and FW in the stroke group were also examined in each tract using ROI (CP, PLIC, and cortex) and slice-by-slice analysis approaches. We test the hypothesis that FA_T asymmetry will be higher and FW asymmetry will be lower in stroke as compared to controls in the M1-CST and PMd-CST. We also test the hypothesis that in the stroke group, grip strength will correlate positively with FA_T asymmetry and negatively with FW asymmetry in the M1-CST and PMd-CST.

METHODS

Subjects

The study group consisted of 23 individuals poststroke, all of whom satisfied four inclusion criteria: (1) a single ischemic stroke affecting function in the contralateral hand at least six months prior, (2) able to apply force to a force transducer in the pinch grip configuration, (3) intact sensation to light touch in the contralateral hand, and (4) able to provide informed consent. All procedures were approved by the local Institutional Review Board and conducted according to the Declaration of Helsinki. Each participant provided written informed consent before testing. Age, sex, and other individual characteristics can be found in Table I. Data were also collected from a control group which included 23 age-matched participants. All stroke subjects self-reported right hand dominance prior to stroke. All control subjects self-reported right hand dominance. Age was

TABLE I. Demographics and relevant clinical information for individuals poststroke

Subject	Age (years)	Sex	Lesion volume (mm^3)	M1-CST lesion overlap (%)	PMd-CST lesion overlap (%)	Time since stroke (years)	Affected hemisphere	UE-FMA motor score	FMA sensation	MAS median	MMSE	Imp MVC (N)	Uni MVC (N)	Grip strength asymmetry
1	55	M	16378	11.73	64.12	4.3	R	30	4	0	30	20	80	0.60
2	57	M	7657	32.33	64.71	9.61	R	26	10	1	30	35	96	0.47
3	46	M	17061	2.71	4.83	4.6	L	9	11	2	28	48.4	92.4	0.31
4	67	F	185	0.00	0.00	1.52	R	62	12	1	30	39.6	44	0.05
5	63	M	15809	0.50	0.00	12.42	L	49	12	1	27	26.4	83.6	0.52
6	72	F	6112	0.00	0.00	3.41	R	51	7	0	29.5	46.25	52.8	0.07
7	52	M	148	8.19	8.86	0.73	L	45	8	1	30	44	88	0.33
8	61	F	52	4.35	35.68	7.96	L	59	9	0	30	62	53	−0.08
9	79	M	2089	14.48	30.11	10.21	L	62	9	0	29	84	70	−0.09
10	31	M	671	0.00	0.00	5.53	R	19	10	3	29.5	11	101.2	0.80
11	76	F	313	1.49	24.52	2.67	L	64	12	0	30	66	44	−0.20
12	56	M	43	51.78	73.87	24.45	L	30	7	0	24	35	58	0.25
13	77	M	1561	2.17	13.37	12.48	L	10	12	0	30	12	50.8	0.62
14	59	M	5093	1.32	25.87	17.65	L	51	12	0	27	48	47	−0.01
15	52	F	398	3.77	0.00	12.1	L	26	12	3	22	3.5	44	0.85
16	65	M	2766	1.34	18.40	5.59	L	30	12	3	30	30.8	70.4	0.39
17	60	F	17687	22.30	59.95	12.52	L	25	12	2	24	5.8	65	0.84
18	75	F	913	33.36	65.82	4.67	R	30	12	1	30	10	57.2	0.70
19	73	M	782	6.03	1.91	4.94	L	58	12	0	27	79.2	57.2	−0.16
20	64	M	7195	21.69	19.85	9.66	L	65	12	0	30	44	66	0.20
21	50	F	348	12.76	26.18	1.65	L	61	9	0	30	44	74.8	0.26
22	58	M	3039	0.05	0.00	2.75	R	40	12	3	30	30.8	70.4	0.39
23	67	M	6269	0.24	0.00	7.42	L	65	12	0	30	35	92	0.45
Mean	**61.52**	**15M/8F**	**4894.3**	**10.11**	**23.39**	**7.78**	**16L/7R**	**42.04**	**10.43**	**0.91**	**28.57**	**37.42**	**67.73**	**0.33**
SD	**11.4**		**6068.31**	**13.68**	**25.45**	**5.72**		**18.45**	**2.23**	**1.16**	**2.35**	**21.91**	**18.05**	**0.32**

Mean values and standard deviations are reported.

Abbreviations: SD, standard deviation; M, male; F, female; L, left; R, right; UE-FMA, upper extremity Fugl–Meyer assessment; MAS, modified Ashworth scale; MMSE, mini mental state exam; Imp, impaired; Uni, unimpaired; MVC, maximum voluntary contraction.

not significantly different between groups [$t(44) = 0.66$; $P = 0.507$] and control subjects (range: 45–80 years) were well-matched to the individuals poststroke (range: 31–79 years) for both age and sex (15M/8F for both groups).

Behavioral Assessments

Each individual's maximum voluntary pinch grip contraction force (MVC) was measured for each hand. Participants were asked to maintain their MVC for three consecutive 5 second trials. Each trial was separated by a 60 s period of rest. The MVC was calculated as the average of the three 5 s trials. For the stroke group, the average MVC for the impaired hand (37.42 ± 21.91N) was significantly less ($P < 0.001$) than the average MVC for the less-impaired hand (67.73 ± 18.05N), hereafter referred to as the unimpaired hand. The nondominant hand in controls will be referred to as the impaired hand and the dominant hand as the unimpaired hand. Grip strength asymmetry was calculated for all stroke and all control subjects using the same formula $[(MVC_{unimpaired} - MVC_{impaired})/(MVC_{unimpaired} + MVC_{impaired})]$. For all stroke subjects, MVC values for each hand are shown in Table I. Positive grip strength asymmetry values reflect greater strength in the unimpaired, compared to the impaired, hand. The severity of upper extremity motor impairment was assessed for each individual poststroke using the upper-extremity section of the Fugl-Meyer Assessment (UE-FMA) [Fugl-Meyer et al., 1975; Gladstone et al., 2002]. Hemiparetic severity (UE-FMA – mean: 42.04; range: 9–65/66 points), grip strength asymmetry (mean: 0.33; range: −0.2 to 0.85), and stroke chronicity (mean: 7.76 years; range 0.73–24.45 years) captured a wide range, representative of motor impairment in individuals poststroke who seek rehabilitation.

MRI Acquisition and Data Processing

Magnetic resonance images were collected using a 32 channel head coil within a 3 T magnetic resonance scanner (Achieva, Best, The Netherlands). Diffusion MRI images were collected from each participant (TR: 7748 ms, TE: 86 ms, flip angle: 90°, field of view: 224 × 224 mm, resolution: 2 mm isotropic, 64 noncollinear diffusion directions, b value of 1,000 s/mm^2 and one with a b value of 0 s/mm^2, 75 axial slices covered the cortex and brainstem). Prior to processing, the diffusion MRI volumes of 7 individuals with lesions in the right hemisphere (Table I) were flipped along the mid-sagittal plane, to produce the same coordinates for the lesioned hemisphere of participants [Archer et al., 2016; Lindenberg et al., 2012; Wang et al., 2012]. FSL (fsl.fmrib.ox.ac.uk) was used for all diffusion MRI data analyses [Jenkinson et al., 2012; Smith et al., 2004; Woolrich et al., 2009]. The diffusion data were first corrected for eddy currents, then for head motion using a 3-D affine registration, after which the brain was extracted [Smith, 2002]. The motion and eddy current corrected volume was then used as input in two different procedures: (1) DTIFIT to calculate FA maps, and (2) custom written MATLAB (R2013a, The Mathworks, Natick, MA, USA) code [Pasternak et al., 2009] to calculate free-water (FW) and FW-corrected FA maps (FA_T). Calculation of FW and FA_T was consistent with prior work [Ofori et al., 2015; Pasternak et al., 2009]. The bi-tensor model predicts signal attenuation in the presence of FW contamination. It represents the sum of attenuations contributed by two different compartments: one that models FW, and a second tissue compartment that models water molecules in the vicinity of tissue membranes. The FW maps are the fractional volume of the FW compartment. The tissue compartment follows DTI's formalism [Basser and Pierpaoli, 1996], where the attenuation is parameterized by a diffusion tensor, leading to corrected DTI measures, such as fractional anisotropy (FA) of the tissue compartment (FA_T). Finding the FW parameter and the corrected diffusion tensor that best fit the acquired signal is described in detail in previous work [Pasternak et al., 2009].

To obtain a standardized space representation of the FW and FA_T maps, the original FA map was registered to the FMRIB FA template in standard space ($1 \times 1 \times 1$ mm) by an affine transformation with 12 degrees of freedom and trilinear interpolation using FLIRT [Jenkinson et al., 2002; Jenkinson and Smith, 2001]. The lesion was masked out during this step to prevent lesion related inaccuracies of transformations. This step resulted in a linear transformed FA map and its corresponding transformation matrix. Linear transformation was followed by a nonlinear transformation (FNIRT) [Jenkinson et al., 2012; Smith et al., 2004; Woolrich et al., 2009], in which the input was the original FA map and the FLIRT transformation matrix. Similar to the FLIRT procedure, the lesion was masked out during this step to prevent lesion related inaccuracies of transformations. The output of this step was the standardized space representation of the FA map and the corresponding nonlinear coefficient file which was subsequently applied to the original FW and FA_T maps to obtain a standardized space representation map for each measure.

Lesion Characterization

For the stroke group, each individual's lesion was manually drawn by two separate drawers for each stroke participant using the FA map in original space. Inter-rater reliability of manual lesion drawing was assessed using intraclass correlation coefficients (ICC) between the two drawers. The ICC was high for all variables, including FA_T (ICC = 0.84), FW (ICC = 0.88), center of mass (ICC = 0.97, 0.80, and 0.97 for x, y, and z, respectively), and volume (ICC = 0.90). As FA_T and FW were our variables of interest, we performed t-tests between FA_T and FW values in each lesion drawn by the two drawers, which did not identify any significant differences for FA_T [$t(44) = 0.15$; $P = 0.88$] or FW [$t(44) = 0.45$; $P = 0.66$]. A standard space representation

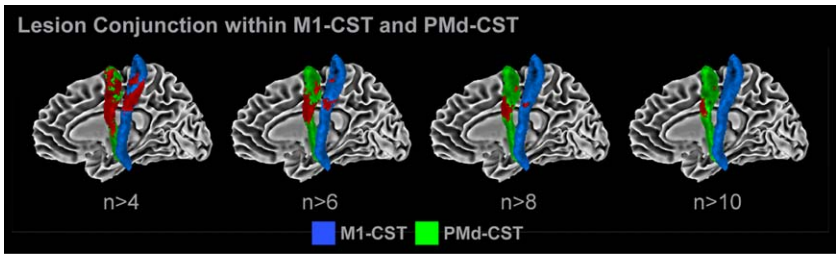

Figure 1.

Lesion conjunction. The lesion conjunction of the M1-CST (blue) and PMd-CST (green) is shown in red. At $n > 4$, much of the tracts are covered by lesions, which indicates that at least four individuals have a stroke in that location. At $n > 6$, $n > 8$, and $n > 10$, there is a steady decrease in volume of M1-CST and PMd-CST covered by lesions. [Color figure can be viewed at wileyonlinelibrary.com]

of each individual's lesion was created using the nonlinear coefficient file obtained from the FA map standardization procedure. Each individual's lesion was then overlaid onto one image to create a lesion conjunction, which was then overlaid on tract templates for the M1-CST and PMd-CST. We used tract templates for the M1-CST and PMd-CST which were identified using probabilistic tractography algorithms that have been outlined elsewhere [Archer et al., 2016]. Figure 1 shows the M1-CST in blue and the PMd-CST in green. There was no overlap between the M1-CST and PMd-CST tracts at $z > 8$. At $z < 8$, there was minimal overlap between tracts (5.53%). Figure 1 shows the lesion conjunction for all individuals in the stroke group within the M1-CST and PMd-CST. Red voxels represent areas of the tract that were directly impacted by a lesion. On the leftmost brain, the lesion conjunction is illustrated using a threshold at $n > 4$, such that red voxels represent lesion locations common to at least 4 individuals. We then increased the threshold to $n > 6$, $n > 8$, and $n > 10$. As shown in Figure 1, at the highest threshold, the spatial extent of common lesion location is reduced and limited to the PMd-CST.

Lesion Masking

The FA_T and FW maps were binarized to create a brain mask for each individual in the stroke group. The lesion was then subtracted from this image to create an image where values of 1 corresponded to areas of the brain not directly impacted by the lesion and values of 0 corresponded to areas of the brain impacted by the lesion. Our primary analyses used asymmetry values to control for within subject variability in FA_T and FW, and are consistent with previous studies using diffusion MRI data [Archer et al., 2016; Lindenberg et al., 2010; Park et al., 2013; Stinear et al., 2007; Wang et al., 2012]. To control for tract volume between hemispheres in the lesion masking analysis, we averaged data from the exact same voxels in each hemisphere. Once the lesion was masked from the tract in the impaired hemisphere, we flipped the masked tract to the nonimpaired hemisphere, so asymmetry values were based on data from the same voxels in both hemispheres. This binarized tract template with the lesion removed was then multiplied with the original FA_T and FW maps to create lesion-masked FA_T and FW maps for each hemisphere. Following this step, there were 4 maps for each individual: unmasked FA_T, unmasked FW, masked FA_T, and masked FW.

Between-Group Differences in FA_T and FW Asymmetry

ROI analysis

Regions of interest (ROI) were created within the M1-CST and PMd-CST for the cerebral peduncle (CP), posterior limb of the internal capsule (PLIC), and cortex. The CP ROI was placed from $z = -7$ to $z = -11$ [Schaechter et al., 2009]. The PLIC ROI was placed from $z = 2$ to $z = 6$ [Archer et al., 2016; Schulz et al., 2012]. The cortex ROI was placed from $z = 51$ to $z = 55$ [Schaechter et al., 2009]. For the M1-CST, lesion load (i.e., lesion overlap) was $3.0 \pm 12.7\%$ for the CP, $1.9 \pm 6.2\%$ for the PLIC, and $10.3 \pm 17.9\%$ for the cortex. For the PMd-CST, lesion load was $3.4 \pm 16.5\%$ for the CP, $3.0 \pm 8.0\%$ for the PLIC, and $21.2 \pm 37.5\%$ for the cortex. For each ROI, 4 asymmetry values (e.g., $[(FW_{unimpaired} - FW_{impaired})/(FW_{unimpaired} + FW_{impaired})]$) were calculated: (1) unmasked FA_T, (2) masked FA_T, (3) unmasked FW, and (4) masked FW. Positive asymmetry scores reflect lower values in the impaired hemisphere. Negative asymmetry scores reflect higher values in the impaired hemisphere. Independent sample t tests were conducted for each measure for each ROI to identify between group differences. Between group differences are reported for P values set at <0.05 uncorrected and $P < 0.05$ corrected for multiple comparisons using the FDR correction [Benjamini and Hochberg, 1995]. All statistical analyses were conducted in SPSS (version 22, Chicago, IL) and MATLAB (R2013a, The Mathworks, Natick, MA, USA).

TABLE II. Mean and standard deviations of impaired and unimpaired FA_T and FW values for stroke and control subjects

	M1-CST			PMd-CST		
	CP	PLIC	Cortex	CP	PLIC	Cortex
			FA_T			
Imp stroke (Unmasked)	0.72 (0.03)	0.69 (0.03)	0.52 (0.03)	0.73 (0.04)	0.70 (0.03)	0.39 (0.04)
Uni stroke (Unmasked)	0.75 (0.08)	0.71 (0.08)	0.59 (0.14)	0.77 (0.14)	0.74 (0.11)	0.57 (0.35)
Imp stroke (Masked)	0.72 (0.03)	0.69 (0.03)	0.55 (0.03)	0.73 (0.04)	0.70 (0.03)	0.46 (0.02)
Uni stroke (Masked)	0.74 (0.08)	0.69 (0.09)	0.55 (0.10)	0.77 (0.14)	0.72 (0.11)	0.34 (0.11)
Imp control	0.73 (0.03)	0.70 (0.02)	0.55 (0.02)	0.75 (0.04)	0.72 (0.04)	0.40 (0.08)
Uni control	0.70 (0.05)	0.68 (0.04)	0.59 (0.05)	0.73 (0.06)	0.71 (0.05)	0.52 (0.07)
			FW			
Imp stroke (Unmasked)	0.16 (0.03)	0.14 (0.03)	0.18 (0.03)	0.13 (0.029)	0.11 (0.03)	0.24 (0.06)
Uni stroke (Unmasked)	0.13 (0.06)	0.09 (0.07)	0.13 (0.04)	0.11 (0.07)	0.08 (0.04)	0.20 (0.13)
Imp stroke (Masked)	0.16 (0.03)	0.13 (0.03)	0.15 (0.03)	0.13 (0.03)	0.11 (0.03)	0.16 (0.01)
Uni stroke (Masked)	0.13 (0.06)	0.10 (0.06)	0.11 (0.04)	0.11 (0.07)	0.08 (0.04)	0.09 (0.04)
Imp control	0.14 (0.03)	0.11 (0.03)	0.13 (0.02)	0.12 (0.03)	0.10 (0.02)	0.17 (0.06)
Uni control	0.11 (0.04)	0.09 (0.05)	0.12 (0.02)	0.10 (0.04)	0.07 (0.03)	0.17 (0.11)

Slice-by-slice analysis

For each tract (M1-CST and PMd-CST), custom-written Linux shell scripts were used to implement a slice-by-slice approach to quantify the FA_T and FW within each slice of each tract in the *z*-axis. The data were collected using 2 mm isotropic voxels, and were then resampled to 1 mm isotropic voxels in MNI space. Slice thickness in *z*-axis for the slice-by-slice analysis was therefore 1 mm. This analysis was conducted in both hemispheres, for both tracts, so that asymmetry values of FA_T and FW could be calculated. For each tract, 4 profiles were created: (1) unmasked FA_T, (2) masked FA_T, (3) unmasked FW, and (4) masked FW. Between-group independent samples *t* tests were conducted at each slice for all four profiles for each tract to determine significant differences. Between group differences are reported using FDR corrected *P* values set at <0.05 and <0.005 [Benjamini and Hochberg, 1995]. FDR correction was calculated for each profile separately. The number of multiple comparisons was therefore equal to the number of slices for each tract (M1-CST: 79 comparisons; PMd-CST: 71 comparisons).

Correlations Between FA_T and FW and Grip Strength in the Chronic Stroke Group

The average FA_T and FW asymmetry scores calculated in the ROI analysis were used as independent variables in a simple regression analysis to predict grip strength asymmetry in the chronic stroke group to determine significant correlations, identified as *P* values <0.05 uncorrected and $P < 0.05$ corrected for multiple comparisons using the FDR correction [Benjamini and Hochberg, 1995]. The FA_T and FW asymmetry in each slice of the M1-CST and PMd-CST were also used as independent variables to predict grip strength asymmetry; thus, we found the slices in which FA_T and FW correlated with grip strength with significance set at $P < 0.05$ uncorrected and $P < 0.05$ corrected for multiple comparisons using the FDR correction [Benjamini and Hochberg, 1995]. Secondary analyses were also conducted to determine whether lesion size, lesion load (within M1-CST and PMd-CST) [Riley et al., 2011], and grip strength asymmetry correlated with FA_T and FW within the entire M1-CST and PMd-CST. To conduct this analysis, an area under the curve (AUC) measure was calculated for each tract by summing the average FA_T or FW values across all slices of the tract. This measure was calculated separately for each subject for the unmasked and masked analysis. Positive AUC values reflect higher FA_T/FW in the unimpaired hemisphere compared to the impaired hemisphere. Conversely, negative AUC values reflect higher FA_T/FW in the impaired hemisphere compared to the unimpaired hemisphere. We expect positive FA_T AUC values and negative FW AUC values in the stroke group.

RESULTS

ROI Analysis: Between-Group Differences in FA_T and FW

Mean FA_T and FW values for each ROI for each hemisphere and each group are shown in Table II. Figure 2A shows the mean ± SEM unmasked FA_T asymmetry scores for the control group (gray) and the stroke group (blue) in the M1-CST. A positive asymmetry score indicates lower FA_T in the impaired hemisphere compared to the unimpaired hemisphere. A negative asymmetry indicates higher FA_T in the impaired hemisphere compared to the unimpaired hemisphere. In the CP and PLIC, the stroke group showed the expected increase in FA_T asymmetry, which

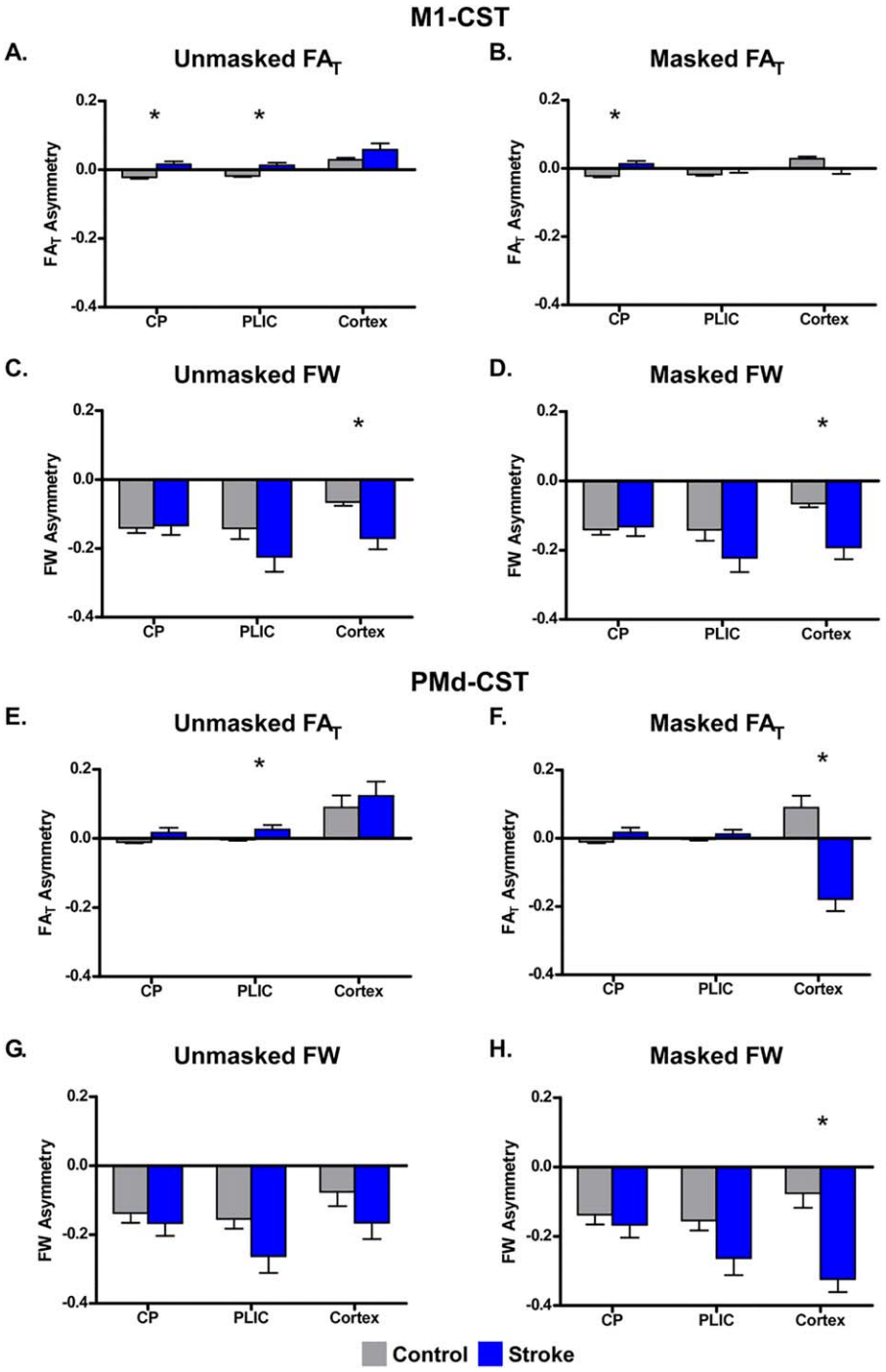

Figure 2.

Between-group differences in FA_T and FW asymmetry within the CP, PLIC, and cortex. Mean FA_T and FW asymmetry is shown for the unmasked (left column) and masked (right column) analyses for the CP, PLIC, and cortex ROIs within M1-CST and PMd-CST for the control (gray) and stroke (blue) groups. Each bar represents the group mean within each ROI, and the error bars represent ±SEM. A positive asymmetry score indicates lower FA_T/FW in the impaired hemisphere compared to the unimpaired hemisphere. A negative asymmetry indicates higher FA_T/FW in the impaired hemisphere compared to the unimpaired hemisphere. [Color figure can be viewed at wileyonlinelibrary.com]

was significantly greater than the negative asymmetry values found in controls [CP: $t(22) = 3.55$; $P < 0.05$, corrected; PLIC: $t(22) = 3.10$; $P < 0.05$, corrected]. FA_T Asymmetry values between groups were of a similar magnitude (0.02) but in different directions. Table II shows that the mean FA_T values in each group differed between hemispheres by 0.03 in CP and 0.02 in PLIC. Figure 2A also shows that for the unmasked analysis, both groups showed a positive FA_T asymmetry score in the cortex. No between-group difference was found. Figure 2B shows the masked FA_T analysis for ROIs in the M1-CST. Lesion masking had little effect on between group differences in the CP [$t(22) = 3.46$; $P < 0.05$, corrected], but abolished the between group difference in PLIC. Indeed, lesion masking attenuated the FA_T asymmetry score in the cortex for the stroke group, such that the groups were no longer significantly different.

Figure 2C,D shows the data from the unmasked and masked FW analyses for the M1-CST. In both analyses, both groups showed a negative asymmetry, which ranged from -0.1 to -0.22. However, as shown in the figure, more negative FW asymmetry was found in the cortex for the stroke compared to the control group for both the unmasked analysis ($t(22) = 3.97$; $P < 0.05$, corrected) and the masked analysis ($t(22) = 3.49$; $P < 0.05$, corrected). Together these data demonstrate that FW is relatively higher in the M1-CST in the impaired hemisphere in the stroke group and is not altered by lesion masking.

Figure 2E–H shows the same plots for the PMd-CST. Similar patterns and similar magnitude were found for both FW and FA_T. As shown in Figure 2E,F, lesion masking abolished the between group difference in FA_T in PLIC, but revealed a significant between group difference in FA_T in the cortex [$t(22) = 5.18$; $P < 0.05$, corrected], with the stroke group moving from a positive asymmetry score to a negative asymmetry score. Figure 2G,H is consistent with the FW data in M1-CST (Fig. 2C,D) and shows that both groups had negative asymmetry scores. However, Figure 2H shows that FW asymmetry was significantly more negative in the stroke group in the cortex when the lesion was masked [$t(22) = 5.40$; $P < 0.05$, corrected], consistent with a relative increase in FW in the impaired hemisphere. Together, these data suggest that between group differences in FA_T asymmetry in CP and PLIC are small and sensitive to direct effects of the lesion itself. Indeed, once the analyses were restricted to nonlesioned tissue, differences in FA_T in CP and PLIC were generally attenuated. In contrast, in the cortex, between-group differences in FW were of a larger magnitude, more pronounced, and maintained or enhanced following lesion masking.

Slice-by-Slice Analysis: Between-Group Differences in FA_T and FW

The unmasked M1-CST FA_T slice-by-slice profile is shown in Figure 3A, in which the black lines represent the group average FA_T asymmetry values (y-axis of plot) at each z-slice (x-axis of plot). Gray shading represents the ± SEM for the control group and blue shading represents the ±SEM for the stroke group. For reference purposes, the slices included in each ROI reported above are demarcated by the yellow lines and yellow labels on the x-axis. In Figure 3A, the tract starts at $z = -14$ within the cerebral peduncle and terminates in the cortex at $z = 64$. Positive asymmetry scores represent lower FA_T in the impaired hemisphere as compared to the unimpaired hemisphere. For the control group, asymmetry is between 0 and -0.1 from $z = -14$ to $z = 36$ and begins to increase to between 0 and 0.1 in the cortex. For the stroke group, FA_T asymmetry is around 0 between $z = -14$ to $z = 20$. At $z = 20$, there is a sharp increase in asymmetry values in the stroke group reflecting a marked reduction in FA_T in the impaired hemisphere compared to the unimpaired hemisphere. This increase in asymmetry peaks at $z = 30$ and a steady reduction in FA_T asymmetry then persists until $z = 40$. From $z = 40$ to $z = 64$, FA_T fluctuates between 0 and 0.1 and is relatively stable in the stroke group. At each slice, an independent t test was performed to examine between group differences in FA_T asymmetry. Significant group differences (FDR corrected) are indicated with a horizontal line above the plot (red: $P < 0.05$; orange: $P < 0.005$). The red lines above Figure 3A show that for the unmasked analysis, FA_T asymmetry was significantly different ($P < 0.05$, corrected) between groups in two large portions of the tract ($z = -14$ to $z = 14$ and $z = 17$ to $z = 30$), with the stroke group showing a significant increase in asymmetry compared to controls. The same analysis was conducted on the masked FA_T data and is shown in Figure 3B. Comparing Figure 3A,B, it is evident that the lesion masking abolished the spike in positive asymmetry values between $z = 20$ and $z = 40$ and reduced variability in FA_T asymmetry values for the stroke group across much of the tract. Consistent with the ROI analyses, asymmetry values for both groups were low and fluctuated between -0.05 and 0.05. We identified three portions of the tract that were significantly different between groups ($P < 0.05$, corrected), with the stroke group exhibiting more positive FA_T asymmetry at $z = -14$ to $z = 2$ and $z = 18$ to $z = 20$. In the cortex, the control group exhibited increased FA_T asymmetry from $z = 54$ to $z = 64$. The orange lines above Figure 3B represent the two portions of the tract that were significantly different between the groups at the $P < 0.005$ FDR corrected level, which include $z = -9$ to $z = -6$ and $z = 57$ to $z = 61$.

Unmasked and masked M1-CST FW data are shown in Figure 3C,D, respectively. Across both analyses, the control group had asymmetry values that range from 0 to -0.2 and show a trend toward more positive asymmetry in more superior z-slices. In contrast, FW asymmetry in the stroke group follows a U-shaped pattern with a negative peak at around $z = 30$ with an asymmetry value of around -0.4. The orange lines above the plots show that

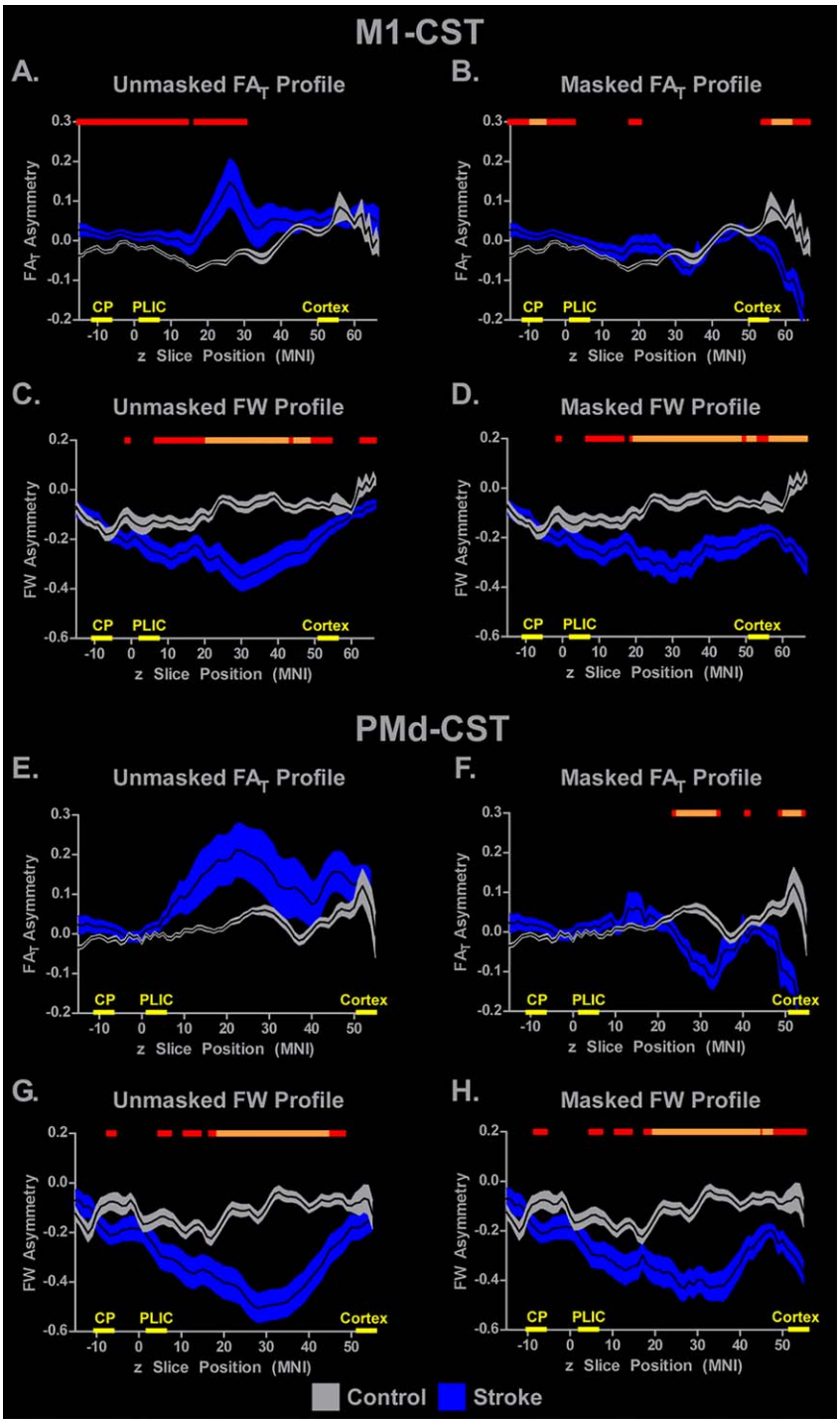

Figure 3.

Slice-by-slice between-group differences in FA_T and FW asymmetry within the M1-CST and PMd-CST. The mean unmasked (left column) and masked (right column) FA_T and FW asymmetry profiles are displayed for M1-CST with a black line, and the gray (control) and blue (stroke) shading represents $\pm$SEM. Comparisons were made between groups for each analysis, with $P < 0.05$, FDR corrected represented with red horizontal lines in each plot and $P < 0.005$, FDR corrected represented with orange horizontal lines. The locations of the CP, PLIC, and cortex ROIs used in the ROI analysis are shown on the *x*-axis. [Color figure can be viewed at wileyonlinelibrary.com]

TABLE III. Correlation coefficients between dMRI measures and maximum grip strength

	M1-CST		PMd-CST	
	Unmasked	Masked	Unmasked	Masked
CP FA_T	0.379*	0.472*	0.450*	0.450*
PLIC FA_T	0.409*	0.488*	0.434*	0.434*
Cortex FA_T	0.165	−0.190	0.407*	−0.266
CP FW	−0.124	−0.139	0.165	0.165
PLIC FW	−0.136	−0.150	0.072	0.072
Cortex FW	**−0.538***	**−0.620***	−0.420*	**−0.578***

*Indicates significance at $P < 0.05$. Bolded r values represent correlations that remained significant ($P < 0.05$) following FDR correction.

FW in large portions of the profile were significantly different between groups. In addition, when comparing Figure 3C,D, it is clear that the effect of lesion masking is minimal, and that the between group differences are notably absent from the CP and PLIC regions that were examined in the ROI analyses.

Figure 3E,F shows the unmasked and masked FA_T profiles for the PMd-CST. The pattern is similar to that shown in the M1-CST (Fig. 3A,B). Increased positive FA_T asymmetry values and increased variability were observed in the stroke group for the unmasked analysis (Fig. 3E), which were attenuated when the lesion was masked (Fig. 3F). Figure 3F shows a significantly more negative asymmetry ($P < 0.005$, FDR corrected) in FA_T for the stroke group in two regions of the tract between $z = 25$ and $z = 32$, and between $z = 50$ and $z = 53$. FW profiles for PMd-CST show that asymmetry values in controls were relatively consistent and varied between 0 and −0.2 across much of the tract, whereas the stroke group showed a U-shaped pattern with a negative peak at around $z = 30$ with an amplitude between −0.4 and −0.6. The negative peak was shallower following lesion masking, but still reached −0.4. The orange lines above the profiles show that significant between-group differences remained in large portions of the tract irrespective of lesion masking.

ROI Analysis: Correlations Between Grip Strength and FAT and FW in CP, PLIC, and Cortex

FA_T and FW values were extracted from the CP, PLIC, and cortex ROIs for each stroke participant for the unmasked and masked analyses. We then examined the correlation between asymmetry in mean grip force and FA_T and FW measures. Table III shows the r values for all correlations between grip force strength FA_T and FW values for both tracts and for the unmasked and masked analyses. FA_T asymmetry in CP and PLIC of the M1-CST

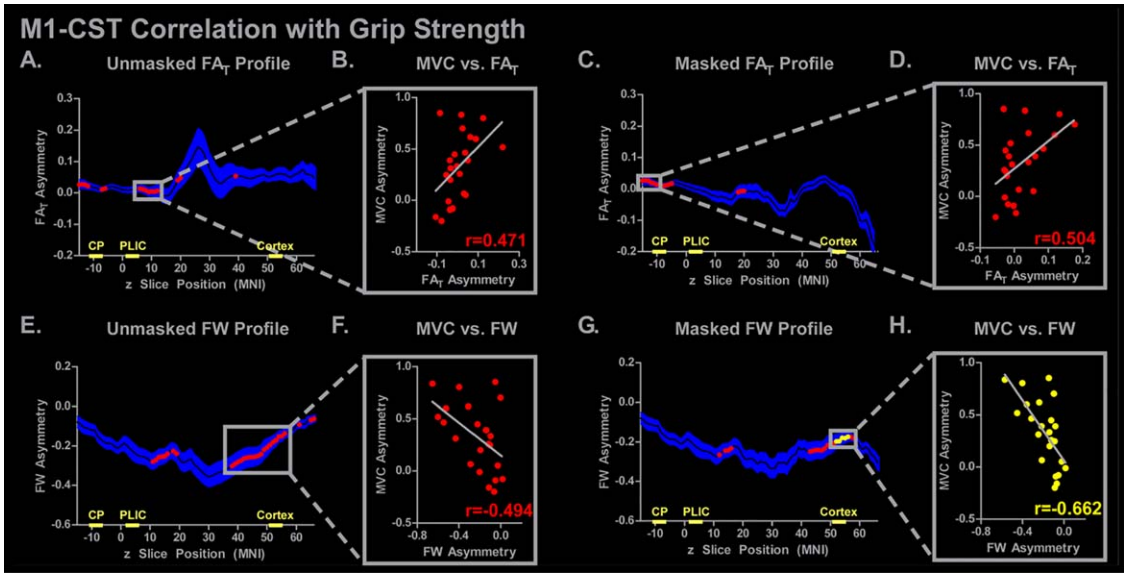

Figure 4.

M1-CST slice-by-slice correlations of FA_T and FW asymmetry with grip strength. The mean unmasked and masked FA_T and FW asymmetry profiles are shown for the stroke subjects, in which the mean is represented with a black line and the blue shading representing ±SEM. Simple regression was performed at each axial slice, and significant correlations are shown with red ($P < 0.05$) or yellow ($P < 0.05$, FDR corrected) dots. The plot to the right of each profile demonstrates the FA_T/FW asymmetry with grip strength asymmetry (MVC). The correlation coefficient for each simple regression is shown. The locations of the CP, PLIC, and cortex ROIs used in the ROI analysis are shown on the x-axis. [Color figure can be viewed at wileyonlinelibrary.com]

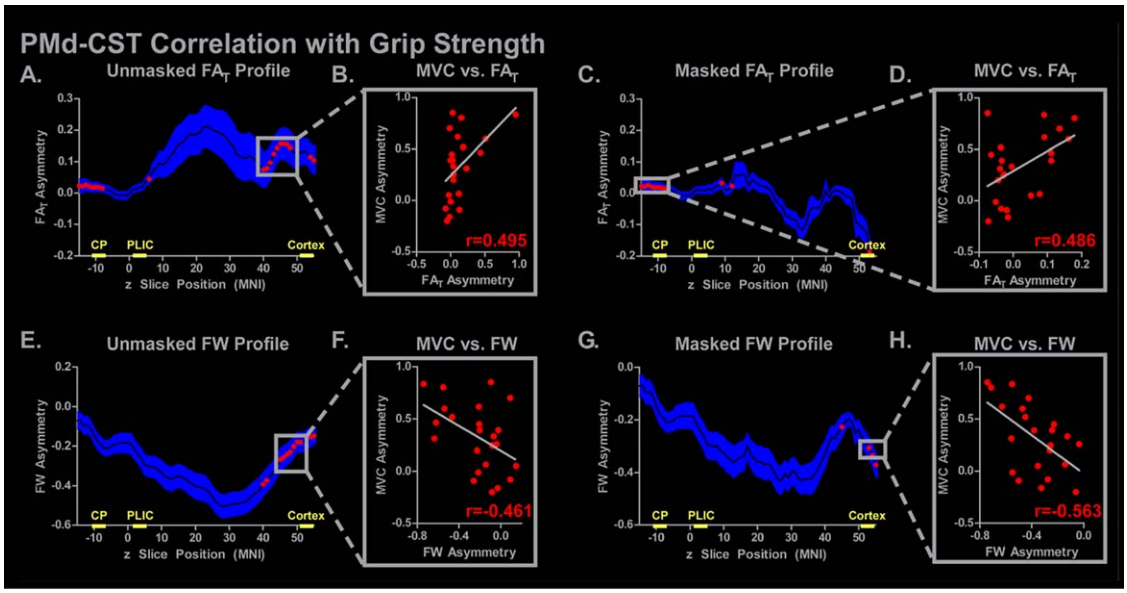

Figure 5.

PMd-CST slice-by-slice correlations of FA_T and FW asymmetry with grip strength. The mean unmasked and masked FA_T and FW asymmetry profiles are shown for the stroke subjects, in which the mean is represented with a black line and the blue shading representing ±SEM. Simple regression was performed at each axial slice, and significant correlations are shown with red ($P < 0.05$) or yellow ($P < 0.05$, FDR corrected) dots. The plot to the right of each profile demonstrates the FA_T/FW asymmetry with grip strength asymmetry (MVC). The correlation coefficient for each simple regression is shown. The locations of the CP, PLIC, and cortex ROIs used in the ROI analysis are shown on the *x*-axis. [Color figure can be viewed at wileyonlinelibrary.com]

were positively correlated with grip strength ($P < 0.05$, uncorrected), but did not survive $P < 0.05$ FDR correction. In contrast, FW asymmetry in the cortical ROI of the M1-CST correlated negatively with grip force strength for both the masked and unmasked analyses ($P < 0.05$, corrected). Significant correlations were not found for grip force asymmetry and FW asymmetry in CP or PLIC.

Correlations between grip force asymmetry and FA_T and FW measures in the PMd-CST ROIs followed a similar pattern as in the M1-CST ROIs. FA_T asymmetry in CP and PLIC of the PMd-CST were positively correlated with grip strength asymmetry ($P < 0.05$, uncorrected), although neither of these correlations survived FDR correction. FW asymmetry in the cortical ROI of the PMd-CST correlated negatively with grip force strength for both the masked and unmasked analyses, with only the masked analysis surviving FDR correction ($P < 0.05$, corrected). Notably, all significant FA_T asymmetry correlations were positive and all significant FW asymmetry correlations were negative.

Slice-by-Slice Analysis: FA_T and FW Correlations With Grip Strength

The unmasked and masked M1-CST FA_T and FW profiles for the stroke group are shown in Figure 4. At each slice, measures of FA_T asymmetry (Fig. 4A–D) and measures of FW (Fig. 4E–H) were used to predict grip strength asymmetry. Red ($P < 0.05$, uncorrected) and yellow ($P < 0.05$, FDR corrected) dots overlaid on the mean asymmetry values indicate slices in which the asymmetry values correlated with asymmetry in grip force strength. Figure 4A shows the unmasked M1-CST FA_T profile and its corresponding correlations at each slice. The gray box in Figure 4B shows the simple regression plot based on the mean FA_T value from a series of slices which demonstrated significant correlations. The plot in Figure 4B shows that more positive FA_T asymmetry is associated with more positive grip strength asymmetry ($r = 0.471$; $P < 0.05$, uncorrected). This pattern is consistent with the position that decreased grip force strength in the more impaired limb is associated with decreased FA_T values in the impaired hemisphere. The same analysis was conducted for FA_T in the M1-CST following lesion masking, and this is shown in Figure 4C,D. Positive correlations were observed in inferior regions of the tract including the CP, although no slice survived FDR correction.

Figure 4E–H shows the correlations between grip force asymmetry and FW asymmetry across the M1-CST profile. In contrast to the FA_T correlations, FW correlations were negative and more prevalent in the cortex, with a series of slices in the cortex in the masked analysis surviving FDR correction (yellow dots in Fig. 4G,H: $r = -0.662$; $P < 0.05$, FDR corrected). This pattern in the data is consistent with

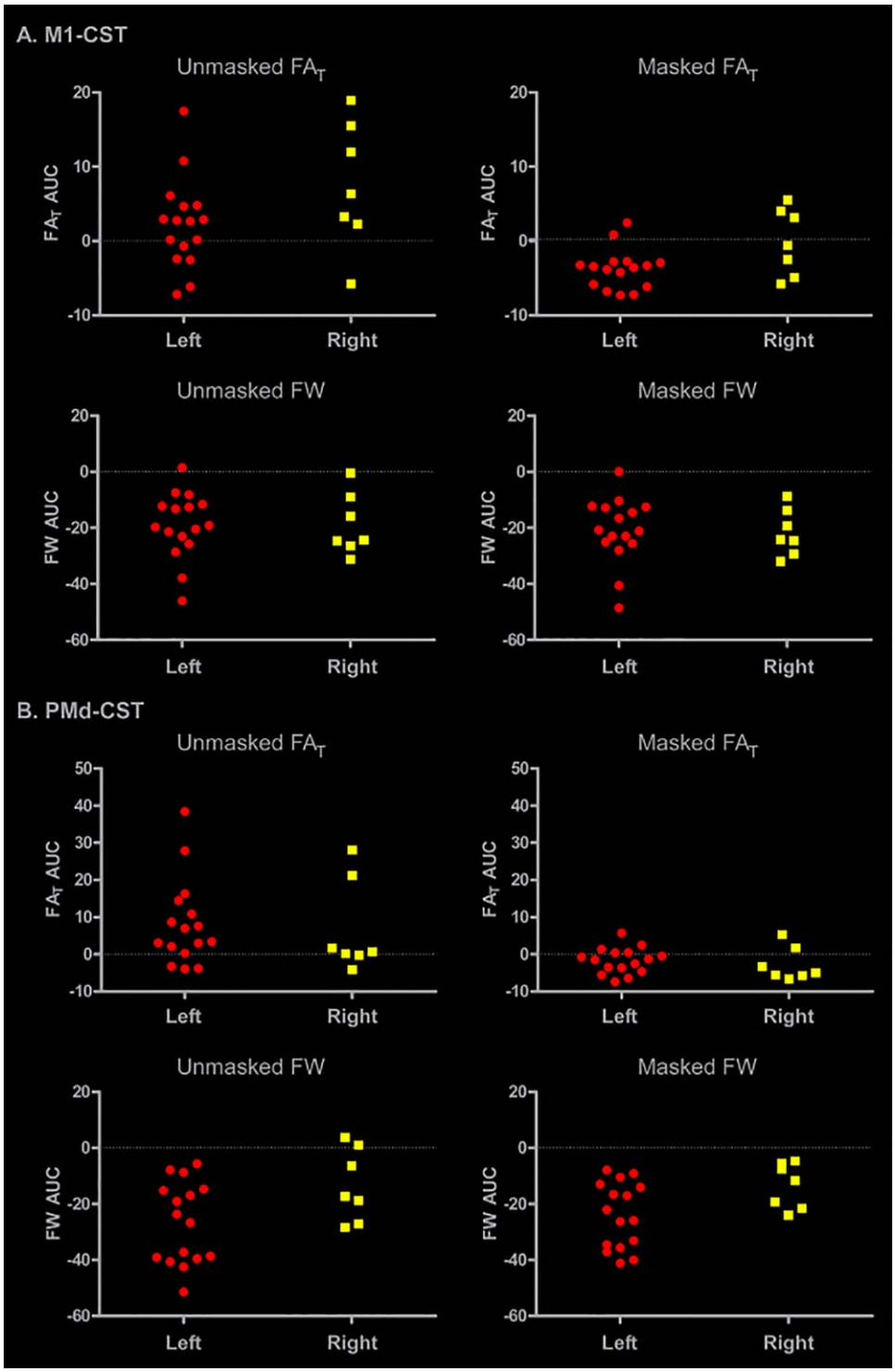

Figure 6.

Effect of lesion side on AUC of FA_T and FW profiles. The stroke group was partitioned into two groups to examine the potential influence of lesion side on our data. AUC values were calculated for each tract (M1-CST, PMd-CST), each measure (FA_T, FW), and each analysis (unmasked, masked). Individuals with a lesion in the left hemisphere are represented by red circles, and individuals with a lesion to the right hemisphere are represented by yellow squares. [Color figure can be viewed at wileyonlinelibrary.com]

TABLE IV. Correlations of unmasked and masked FA_T and FW asymmetry area under the curve (AUC) measures with lesion size, lesion load, and grip strength asymmetry

	Unmasked area under the curve				Masked area under the curve				Grip strength asymmetry
	M1 FA_T	PMd FA_T	M1 FW	PMd FW	M1 FA_T	PMd FA_T	M1 FW	PMd FW	
Lesion size	**0.669**	0.085	**−0.780**	**−0.714**	**0.769**	0.399	**−0.657**	−0.345	0.247
M1-CST lesion load	**0.749**	-	**−0.746**	-	**0.869**	-	**−0.771**	-	0.147
PMd-CST lesion load	-	0.023	-	**−0.748**	-	0.431	-	−0.419	0.144

Bolded correlation coefficients indicate FDR corrected significance ($P < 0.05$).

the correlations observed in the analysis for FW in the Cortical ROI in the M1-CST, and demonstrates that higher FW in the impaired hemisphere is associated with lower grip-strength in the impaired limb.

The unmasked and masked PMd-CST FA_T and FW asymmetry profiles for the stroke group are shown in Figure 5. Figure 5A–D shows that FA_T asymmetry was positively correlated with grip force asymmetry in the CP and cortex for the unmasked analysis, and in the CP region for the masked analysis. However, no FA_T correlation at the slice level survived FDR correction. Negative correlations between FW and grip strength were more prevalent in the cortex of the PMd-CST in both the unmasked and the masked lesion analyses, but no correlation survived FDR correction.

To determine whether lesion side played a role in our data, we partitioned the stroke subjects into two groups. Figure 6 shows the data for individuals with left hemisphere lesions ($N = 16$: red circles) and individuals with right hemisphere lesions ($N = 7$: yellow squares). We calculated the area under the curve (AUC) for the FA_T and FW asymmetry profiles for the M1-CST and the PMd-CST for the masked and the unmasked analysis. The data show a similar pattern across each subset of stroke subjects, and are consistent with the ROI and slice-by-slice analyses in showing a pronounced effect of lesion masking on FA_T but not FW. Figure 6 suggests that there is no strong effect of lesion side on the data.

To determine whether FA_T and FW AUC and grip force asymmetry were related to lesion size and lesion load, we computed tract specific correlations between these variables. Table IV shows the corresponding correlation coefficients for each AUC value from the masked analysis and the unmasked analysis. Lesion size and lesion load of the M1-CST correlated positively with FA_T AUC and negatively with FW AUC. These effects were similar for the unmasked and masked analyses. Lesion size and PMd-CST lesion load were negatively correlated with PMd FW AUC. Neither lesion size nor lesion load predicted grip strength asymmetry.

DISCUSSION

Measures from diffusion magnetic resonance imaging have been used to characterize the corticospinal tract in the chronic phase after stroke. However, diffusion measurements can be influenced by partial volume effects from free water, the spatial location in which the measurement is taken, and lesion masking. This study addressed each of these issues and produced three novel findings. First, following lesion masking and correction for multiple comparisons, relative increases in FW were found for the stroke group in large portions of the M1-CST and PMd-CST in the lesioned hemisphere. Second, FW in cortical regions was the best predictor of grip strength asymmetry in the stroke group. Third, our findings also demonstrated that FA_T is sensitive to the direct effect of the lesion itself, and that once the lesion is controlled for, differences in FA_T in nonlesioned tissue were small and generally similar between hemispheres and groups. Taken together, our observations suggest that FW is a robust biological measurement that can be used to assess residual, nonlesioned CST white matter after stroke.

Identifying biomarkers for recovery after stroke continues to gain traction in the literature [Burke Quinlan et al., 2015; Hirai et al., 2016; Kim and Winstein, 2016; Stinear et al., 2012]. Biomarkers based on structural neuroimaging are an attractive option because data collection does not rely on one's ability to complete a functional task. Conventional stroke-related diffusion MRI studies have used single tensor models to show that FA is reduced in the CP and PLIC in the chronic phase after stroke [Archer et al., 2016; Lindenberg et al., 2010, 2012; Stinear et al., 2007, 2012]. Lower FA values in regions of the CST beyond the lesion have been interpreted as reflecting Wallerian degeneration [Thomalla et al., 2005]. However, uncorrected FA measurements reflect a combination of tissue microstructure and free water; the presence of free water will typically attenuate the FA measurement [Metzler-Baddeley et al., 2012; Reetz et al., 2013]. In this study, we addressed this issue by using a bi-tensor model to calculate FW and FA_T. Observations from our ROI analyses add to previous findings by demonstrating that, relative to controls, FA_T asymmetry in the stroke group was increased in PLIC in the M1-CST and PMd-CST before lesion masking. Lesion masking abolished the between group differences, however, which suggests that they were driven by the direct effects of the lesion itself. FA_T in the CP of M1-CST also showed increased asymmetry in the stroke group irrespective of lesion masking. Our findings in CP and PLIC are

important for two reasons. First, when the lesion is not masked, we show that stroke-related changes in PLIC and CP are associated with relative decreases in FA_T rather than an increase in FW in the lesioned hemisphere, which clarifies previous findings that FA is reduced in these subcortical regions in the chronic phase after stroke [Archer et al., 2016; Lindenberg et al., 2010, 2012; Stinear et al., 2007, 2012]. One interpretation of this finding is that unmasked FA_T values reflect Wallerian degeneration such as fibrosis and tract atrophy in the stroke group [DeVetten et al., 2010; Iizuka et al., 1989; Johnson et al., 1950; Lampert and Cressman, 1966; Mazumdar et al., 2003]. A second interpretation is that these effects reflect the direct effect of the lesion itself. For instance, lesion masking of our ROI analyses abolished 2 of the 3 significant between group asymmetry differences in CP and PLIC, which suggests that masking the lesion plays a significant role in identifying between group differences. Caution should therefore be exercised when interpreting increased FA asymmetry as reflecting decreases in tissue microstructure in the impaired hemisphere if the lesion has not been masked. Indeed, our observations show that lesion masking generally reduced positive FA_T asymmetry values in the stroke group, moving them closer to the asymmetry scores in controls and in some instances moving the asymmetry score negative. Our observations suggest that in subcortical structures, the tissue that did remain after lesion masking was not consistently different from the nonlesioned tissue in the same voxels in the unimpaired hemisphere.

A strength of using asymmetry scores is that they control for individual differences in FA values between subjects. Differences in FA_T between hemispheres in CP and PLIC were on the order of 0.03, which is a relatively small change given the absolute range of 0.68–0.75 within these regions. Other studies have reported asymmetry values in the range of −0.1 to 0.8, but these scores were derived from uncorrected FA values, and it is not clear whether lesions were masked [Lindenberg et al., 2010; Stinear et al., 2007, 2012]. Together, the current findings demonstrate that the direct effects of the lesion on white matter microstructure are better characterized by changes in tissue as compared to free water within subcortical areas where fiber convergence is high. However, differences in asymmetry scores within these ROIs were low, and were driven by relatively small changes in the absolute FA_T values between hemispheres and between groups. FA_T asymmetry scores were also sensitive to the direct effect of the lesion itself, and once the lesion was masked, the intact tissue generally resembled tissue in the nonlesioned hemisphere.

FW asymmetry scores were negative in all groups in all ROIs and were more sensitive to between group differences in the cortex. After lesion masking, greater negative asymmetry was found for the stroke group relative to the control group, which is consistent with the position that FW was higher in the impaired as compared to the unimpaired hemisphere. Consistent with previous literature [Ofori et al., 2015; Pasternak et al., 2012b], raw free-water values ranged from 0.08 to 0.20, and differences between hemispheres were on the order of 0.01 to 0.03. These between hemisphere differences represent a much larger relative change in the FW measurements as compared to the FA_T measurements, which are reflected in the larger asymmetry values in the ROI analyses. Our FW asymmetry scores as compared to our FA_T scores were more similar in magnitude to previous studies which assessed uncorrected FA asymmetry [Lindenberg et al., 2010; Stinear et al., 2007, 2012]. One interpretation of this finding is that previous uncorrected FA asymmetry data may have been disproportionally driven by increased FW rather than by decreased tissue microstructure.

Slice-by-slice analyses extended the ROI findings by revealing robust negative FW asymmetry values in large portions of the lesioned hemisphere in both tracts. The pattern in FW profiles was consistent across tracts and across unmasked and masked analyses, and was robust to correction for multiple comparisons. Our data therefore suggest that FW is a stable measurement that is sensitive to lesion-related changes in white matter in large portions of the CST, and should generalize well across studies. Indeed, although stroke-related changes in brain function in cortical motor areas are well established [Cramer et al., 1997; Grefkes et al., 2008; Nouri and Cramer, 2011; Plow et al., 2015; Rehme et al., 2012], much less is known about the effects of stroke on white matter in the motor cortices, as previous studies often focus on subcortical regions such as PLIC and CP. Increases in FW in cortical regions in this study may reflect an increase in neuroinflammation and/or a reduction in cellular density [Pasternak et al., 2012a; Wang et al., 2011] that appears to be specific to regions superior of the PLIC where crossing fibers are most prevalent. Future studies in both human and animal models will be necessary to determine the physiological mechanisms underlying region specific lesion-related changes in FW. Nevertheless, the current data suggest that FW in regions beyond the CP and PLIC may be a useful measurement that is sensitive to lesion-related changes in white matter and is robust when controlling for direct effects of the lesion itself [Hirai et al., 2016; Kim and Winstein, 2016; Stinear et al., 2012]. There is a growing literature on using FW measurements to examine brain microstructure in disease states such as Parkinsonism and schizophrenia [Ofori et al., 2015; Pasternak et al., 2012b]. The current observations are the first to extend this literature to include chronic stroke.

Decreases in CST FA have been associated with decreases in poststroke motor function [Park et al., 2013; Schaechter et al., 2008], with FA in the PLIC correlating positively with measures of motor skill, grip strength, and clinical tests of motor function [Lindenberg et al., 2010, 2012; Schaechter et al., 2008]. Our ROI analyses add to these findings by showing that FA_T correlated positively with grip strength in PLIC and CP. Our findings are

consistent with those of Schulz and colleagues [Schulz et al., 2012] who also found significant positive correlations between grip force and FA in PLIC regions of the M1-CST and PMd-CST. Although correlations between grip force strength and FA_T were consistent across both tracts and were robust to the effects of lesion masking, it is important to note that none of the correlations including CP and PLIC survived correction for multiple comparisons. This pattern was consistent across the ROI analysis and the slice-by-slice analysis. In contrast, FW correlated negatively with grip strength in cortical ROIs in both tracts, with observations in 3 of the 4 cortical ROIs robust to lesion masking and correction for multiple comparisons. Slice-by-slice correlation analyses showed that FW in a cortical region of the M1-CST following lesion masking was the only area to survive corrections for multiple comparisons.

Our data clearly demonstrate that lesion masking reduces variability in the FW and FA_T measures across the CST profiles. This reduction in variability was more prominent for measures of FA_T, where lesion masking generally resulted in the remaining tissue looking more similar to the nonlesioned tissue in the nonimpaired hemisphere. Whereas some dMRI studies report the presence of lesion masking [Lunven et al., 2015], the absence of such a statement suggests that lesion masking is not commonly used [Lindenberg et al., 2012; Schaechter et al., 2009]. Thus, our observations suggest that lesion masking is important and will have a significant impact on measures of tissue microstructure as compared to measures of FW. Another strength of our observations is that the lesion masked analyses of the FW and FA_T profiles sampled the same voxels in both hemispheres. Hence, if a voxel was directly impacted by the lesion in the lesioned hemisphere, the same voxel in the nonlesioned hemisphere was also removed from the analysis. One caveat to the current approach, however, is that differences between the masked and the unmasked analysis cannot be exclusively attributed to changes in the lesioned hemisphere, as the removal of voxels in the nonlesioned side may have also contributed to the change in asymmetry. We did not implement this same voxel matching approach in our ROI analyses.

Great progress has been made in correlating FA to motor function in the chronic phase after stroke, but emerging evidence suggests that FA alone may not be the optimal measure to predict stroke-related changes in motor function across time. For instance, recent evidence shows that FA values measured 1–2 days after stroke are not a strong predictor of motor outcomes 3 months later [Doughty et al., 2016]. One explanation for this finding is that Wallerian degeneration may not begin this early after stroke, and changes in FA are more pronounced as Wallerian degeneration increases over time. Other evidence shows that in the acute phase, FA in PLIC predicts upper limb recovery at 3 months poststroke, but only in individuals in whom a motor evoked potential cannot be recorded [Stinear et al., 2012]. Another study found that while FA is not predictive of motor skill in the acute phase of stroke, it is a strong predictor in the subacute phase [Groisser et al., 2014]. Future studies are necessary to determine whether FW and/or FA_T are more sensitive to changes in brain microstructure in the acute phase after stroke. A consistent structural measure that is not conflated by tissue and free water that can be used longitudinally after stroke to predict motor outcomes and recovery trajectory would represent a significant advance in the literature [Kim and Winstein, 2016].

CONFLICT OF INTEREST

Stephen A. Coombes is the co-founder and manager of Neuroimaging Solutions, LLC.

ACKNOWLEDGMENTS

MRI data collection was supported through the National High Magnetic Field Laboratory and obtained at the Advanced Magnetic Resonance Imaging and Spectroscopy facility in the McKnight Brain Institute of the University of Florida.

REFERENCES

Archer DB, Misra G, Patten C, Coombes SA (2016): Microstructural properties of premotor pathways predict visuomotor performance in chronic stroke. Hum Brain Mapp.

Basser PJ, Pierpaoli C (1996): Microstructural and physiological features of tissues elucidated by quantitative-diffusion-tensor MRI. J Magn Reson B 111:209–219.

Benjamini Y, Hochberg Y (1995): Controlling the false discovery rate: A practical and powerful approach to multiple testing. J R Stat Soc Ser B Methodol 57:289–300.

Buetefisch CM, Revill KP, Shuster L, Hines B, Parsons M (2014): Motor demand-dependent activation of ipsilateral motor cortex. J Neurophysiol 112:999–1009.

Burke Quinlan E, Dodakian L, See J, McKenzie A, Le V, Wojnowicz M, Shahbaba B, Cramer SC (2015): Neural function, injury, and stroke subtype predict treatment gains after stroke. Ann Neurol 77:132–145.

Cramer SC, Nelles G, Benson RR, Kaplan JD, Parker RA, Kwong KK, Kennedy DN, Finklestein SP, Rosen BR (1997): A functional MRI study of subjects recovered from hemiparetic stroke. Stroke 28:2518–2527.

DeVetten G, Coutts SB, Hill MD, Goyal M, Eesa M, O'Brien B, Demchuk AM, Kirton A, Monitor Groups Vs (2010): Acute corticospinal tract Wallerian degeneration is associated with stroke outcome. Stroke 41:751–756.

Doughty C, Wang J, Feng W, Hackney D, Pani E, Schlaug G (2016): Detection and predictive value of fractional anisotropy changes of the corticospinal tract in the acute phase of a stroke. Stroke 47:1520–1526.

Dum RP, Strick PL (1991): The origin of corticospinal projections from the premotor areas in the frontal lobe. J Neurosci 11: 667–689.

Grefkes C, Nowak DA, Eickhoff SB, Dafotakis M, Kust J, Karbe H, Fink GR (2008): Cortical connectivity after subcortical stroke

assessed with functional magnetic resonance imaging. Ann Neurol 63:236–246.
Groisser BN, Copen WA, Singhal AB, Hirai KK, Schaechter JD (2014): Corticospinal tract diffusion abnormalities early after stroke predict motor outcome. Neurorehabil Neural Repair 28:751–760.
He SQ, Dum RP, Strick PL (1993): Topographic organization of corticospinal projections from the frontal lobe: Motor areas on the lateral surface of the hemisphere. J Neurosci 13:952–980.
He SQ, Dum RP, Strick PL (1995): Topographic organization of corticospinal projections from the frontal lobe: Motor areas on the medial surface of the hemisphere. J Neurosci 15:3284–3306.
Heffner RS, Masterton RB (1983): The role of the corticospinal tract in the evolution of human digital dexterity. Brain Behav Evol 23:165–183.
Hirai KK, Groisser BN, Copen WA, Singhal AB, Schaechter JD (2016): Comparing prognostic strength of acute corticospinal tract injury measured by a new diffusion tensor imaging based template approach versus common approaches. J Neurosci Methods 257:204–213.
Iizuka H, Sakatani K, Young W (1989): Corticofugal axonal degeneration in rats after middle cerebral artery occlusion. Stroke 20: 1396–1402.
Jang SH (2009): The role of the corticospinal tract in motor recovery in patients with a stroke: A review. NeuroRehabilitation 24:285–290.
Jenkinson M, Bannister P, Brady M, Smith S (2002): Improved optimization for the robust and accurate linear registration and motion correction of brain images. NeuroImage 17:825–841.
Jenkinson M, Beckmann CF, Behrens TE, Woolrich MW, Smith SM (2012): Fsl. NeuroImage 62:782–790.
Jenkinson M, Smith S (2001): A global optimisation method for robust affine registration of brain images. Med Image Anal 5: 143–156.
Johnson AC, Mc NA, Rossiter RJ (1950): Chemistry of wallerian degeneration. A review of recent studies. Arch Neurol Psychiatry 64:105–121.
Jones DK, Knosche TR, Turner R (2013): White matter integrity, fiber count, and other fallacies: The do's and don'ts of diffusion MRI. NeuroImage 73:239–254.
Kim B, Winstein C (2016): Can neurological biomarkers of brain impairment be used to predict poststroke motor recovery? A systematic review. Neurorehabil Neural Repair.
Lampert PW, Cressman MR (1966): Fine-structural changes of myelin sheaths after axonal degeneration in the spinal cord of rats. Am J Pathol 49:1139–1155.
Lemon RN, Griffiths J (2005): Comparing the function of the corticospinal system in different species: Organizational differences for motor specialization? Muscle Nerve 32:261–279.
Lindenberg R, Renga V, Zhu LL, Betzler F, Alsop D, Schlaug G (2010): Structural integrity of corticospinal motor fibers predicts motor impairment in chronic stroke. Neurology 74:280–287.
Lindenberg R, Zhu LL, Ruber T, Schlaug G (2012): Predicting functional motor potential in chronic stroke patients using diffusion tensor imaging. Hum Brain Mapp 33:1040–1051.
Loubinoux I, Dechaumont-Palacin S, Castel-Lacanal E, De Boissezon X, Marque P, Pariente J, Albucher JF, Berry I, Chollet F (2007): Prognostic value of FMRI in recovery of hand function in subcortical stroke patients. Cereb Cortex 17:2980–2987.
Lunven M, Thiebaut De Schotten M, Bourlon C, Duret C, Migliaccio R, Rode G, Bartolomeo P (2015): White matter lesional predictors of chronic visual neglect: A longitudinal study. Brain 138:746–760.
Mazumdar A, Mukherjee P, Miller JH, Malde H, McKinstry RC (2003): Diffusion-weighted imaging of acute corticospinal tract injury preceding Wallerian degeneration in the maturing human brain. AJNR Am J Neuroradiol 24:1057–1066.
Metzler-Baddeley C, O'Sullivan MJ, Bells S, Pasternak O, Jones DK (2012): How and how not to correct for CSF-contamination in diffusion MRI. NeuroImage 59:1394–1403.
Meyer S, Karttunen AH, Thijs V, Feys H, Verheyden G (2014): How do somatosensory deficits in the arm and hand relate to upper limb impairment, activity, and participation problems after stroke? A systematic review. Phys Ther 94:1220–1231.
Nakayama H, Jorgensen HS, Raaschou HO, Olsen TS (1994): Recovery of upper extremity function in stroke patients: the Copenhagen Stroke Study. Arch Phys Med Rehabil 75:394–398.
Nouri S, Cramer SC (2011): Anatomy and physiology predict response to motor cortex stimulation after stroke. Neurology 77:1076–1083.
Nudo RJ, Masterton RB (1990a): Descending pathways to the spinal cord, III: Sites of origin of the corticospinal tract. J Comp Neurol 296:559–583.
Nudo RJ, Masterton RB (1990b): Descending pathways to the spinal cord, IV: Some factors related to the amount of cortex devoted to the corticospinal tract. J Comp Neurol 296: 584–597.
Ofori E, Pasternak O, Planetta PJ, Burciu R, Snyder A, Febo M, Golde TE, Okun MS, Vaillancourt DE (2015): Increased free water in the substantia nigra of Parkinson's disease: A single-site and multi-site study. Neurobiol Aging 36:1097–1104.
Park CH, Kou N, Boudrias MH, Playford ED, Ward NS (2013): Assessing a standardised approach to measuring corticospinal integrity after stroke with DTI. NeuroImage Clin 2:521–533.
Pasternak O, Shenton ME, Westin CF (2012a): Estimation of extracellular volume from regularized multi-shell diffusion MRI. Med Image Comput Comput Assist Interv 15:305–312.
Pasternak O, Sochen N, Gur Y, Intrator N, Assaf Y (2009): Free water elimination and mapping from diffusion MRI. Magn Reson Med 62:717–730.
Pasternak O, Westin CF, Bouix S, Seidman LJ, Goldstein JM, Woo TU, Petryshen TL, Mesholam-Gately RI, McCarley RW, Kikinis R, Shenton ME, Kubicki M (2012b): Excessive extracellular volume reveals a neurodegenerative pattern in schizophrenia onset. J Neurosci 32:17365–17372.
Plow EB, Cunningham DA, Varnerin N, Machado A (2015): Rethinking stimulation of the brain in stroke rehabilitation: Why higher motor areas might be better alternatives for patients with greater impairments. Neuroscientist 21:225–240.
Reetz K, Binkofski F (2013): Ataxia. In: Tuite P, Dagher A, editors. Magnetic Resonance Imaging in Movement Disorders. New York: Cambridge University Press.
Reetz K, Costa AS, Mirzazade S, Lehmann A, Juzek A, Rakowicz M, Boguslawska R, Schols L, Linnemann C, Mariotti C, Grisoli M, Durr A, van de Warrenburg BP, Timmann D, Pandolfo M, Bauer P, Jacobi H, Hauser TK, Klockgether T, Schulz JB (2013): Genotype-specific patterns of atrophy progression are more sensitive than clinical decline in SCA1, SCA3 and SCA6. Brain 136:905–917.
Rehme AK, Eickhoff SB, Rottschy C, Fink GR, Grefkes C (2012): Activation likelihood estimation meta-analysis of motor-related neural activity after stroke. NeuroImage 59:2771–2782.
Riley JD, Le V, Der-Yeghiaian L, See J, Newton JM, Ward NS, Cramer SC (2011): Anatomy of stroke injury predicts gains from therapy. Stroke 42:421–426.

Schaechter JD, Fricker ZP, Perdue KL, Helmer KG, Vangel MG, Greve DN, Makris N (2009): Microstructural status of ipsilesional and contralesional corticospinal tract correlates with motor skill in chronic stroke patients. Hum Brain Mapp 30: 3461–3474.

Schaechter JD, Perdue KL, Wang R (2008): Structural damage to the corticospinal tract correlates with bilateral sensorimotor cortex reorganization in stroke patients. NeuroImage 39:1370–1382.

Schulz R, Park CH, Boudrias MH, Gerloff C, Hummel FC, Ward NS (2012): Assessing the integrity of corticospinal pathways from primary and secondary cortical motor areas after stroke. Stroke 43:2248–2251.

Smith SM (2002): Fast robust automated brain extraction. Hum Brain Mapp 17:143–155.

Smith SM, Jenkinson M, Woolrich MW, Beckmann CF, Behrens TE, Johansen-Berg H, Bannister PR, De Luca M, Drobnjak I, Flitney DE, Niazy RK, Saunders J, Vickers J, Zhang Y, De Stefano N, Brady JM, Matthews PM (2004): Advances in functional and structural MR image analysis and implementation as FSL. NeuroImage 23: S208–S219.

Stinear CM, Barber PA, Petoe M, Anwar S, Byblow WD (2012): The PREP algorithm predicts potential for upper limb recovery after stroke. Brain 135:2527–2535.

Stinear CM, Barber PA, Smale PR, Coxon JP, Fleming MK, Byblow WD (2007): Functional potential in chronic stroke patients depends on corticospinal tract integrity. Brain 130:170–180.

Tennant A, Geddes JM, Fear J, Hillman M, Chamberlain MA (1997): Outcome following stroke. Disabil Rehabil 19:278–284.

Thomalla G, Glauche V, Koch MA, Beaulieu C, Weiller C, Rother J (2004): Diffusion tensor imaging detects early Wallerian degeneration of the pyramidal tract after ischemic stroke. NeuroImage 22:1767–1774.

Thomalla G, Glauche V, Weiller C, Rother J (2005): Time course of wallerian degeneration after ischaemic stroke revealed by diffusion tensor imaging. J Neurol Neurosurg Psychiatry 76: 266–268.

Tombari D, Loubinoux I, Pariente J, Gerdelat A, Albucher JF, Tardy J, Cassol E, Chollet F (2004): A longitudinal fMRI study: In recovering and then in clinically stable sub-cortical stroke patients. NeuroImage 23:827–839.

Wang LE, Tittgemeyer M, Imperati D, Diekhoff S, Ameli M, Fink GR, Grefkes C (2012): Degeneration of corpus callosum and recovery of motor function after stroke: A multimodal magnetic resonance imaging study. Hum Brain Mapp 33: 2941–2956.

Wang Y, Wang Q, Haldar JP, Yeh FC, Xie M, Sun P, Tu TW, Trinkaus K, Klein RS, Cross AH, Song SK (2011): Quantification of increased cellularity during inflammatory demyelination. Brain 134:3590–3601.

Ward NS, Brown MM, Thompson AJ, Frackowiak RS (2003): Neural correlates of outcome after stroke: A cross-sectional fMRI study. Brain 126:1430–1448.

Woolrich MW, Jbabdi S, Patenaude B, Chappell M, Makni S, Behrens T, Beckmann C, Jenkinson M, Smith SM (2009): Bayesian analysis of neuroimaging data in FSL. NeuroImage 45: S173–S186.